INFLUENCE OF ALR ON DISINTEGRATION CHARACTERISTICS IN PNEUMATIC SPRAY

S. G. LEE[1], B. C. JOO[2], K. C. KIM[2] and B. J. RHO[3]*

[1]Research Institute of Industrial Technology, Chonbuk National University
[2]Dept. of Mechanical Engineering, Chonbuk National University
[3]Faculty of Mechanical Engineering, Chonbuk National University & AHTRI, Chonbuk 561-756, Korea

ABSTRACT−The droplet diameters and the turbulent characteristics of a counterflowing internal mixing pneumatic nozzle was mainly focused. The measurements were made using a Phase Doppler Particle Analyzer under the different air pressures. The nozzle with tangential-drilled holes at an angle of 30 to the central axis has been designed. The spatial distributions of velocities, fluctuating velocities, droplet diameters and SMD were quantitatively and qualitatively analyzed. The results indicated that the stronger axial momentum caused the less dispersion radially, and that axial fluctuating velocities were substantially higher than the radial and the tangential ones. This implies that the disintegration process is enhanced with the higher air pressure. The larger droplets were detected near the spray centerline at the upstream while the smaller ones were generated at the downstream. This was attributed to the lower rates of spherical particles which were not subject to instantaneous breakup. However, substantial increases in SMD from the central part toward spray periphery were predictable in downstream regions.

KEY WORDS : ALR (Air to Liquid Mass Flow Ratio), PDPA (Phase Doppler Particle Analyzer), SMD (Sauter Mean Diameter), Two-phase atomizer, Atomization and counter-swirling pneumatic nozzle

1. INTRODUCTION

Two-phase atomizers are utilized very often because of their own advantages such as uniform distributions and appreciable disintegrations in the process of spray. Many attempts of breaking up the liquid into multitudinous droplets have been carried out, using interferometric techniques like PDPA which measures the droplet velocity and size simultaneously for droplets passing through the measurement volume. Turbulent disintegrations are believed to be brought about due to the droplet inter-actions. Aerodynamic effects by the geometric configurations are known to play a significant role in the formation of turbulent mixing. Thus, getting a high momentum is the prerequisites for the good atomization regarding the aerodynamic consideration.

A large number of publications have been described on the disintegration mechanism issuing from the twin-fluid atomizer. Presser C. *et al.* (1996) and Rho *et al.* (1998) analyzed the atomization in the geometrically swirling atomizer. Eroglu *et al.* (1991) and Lefebvre (1992) studied that the SMD and air/liquid mass ratios have a linear correlation.

The aim in this experimental investigation is to describe the turbulent mixing flow and disintegration characteristics from the internal mixing counter-flowing axisymmetric jets.

2. EXPERIMENTAL APPARATUS

The nozzle configuration is schematically shown in Figure 1. The discharge orifice diameter (d_0) is 2 mm, swirl chamber diameter (D_s) is 9 mm and the ratio of the length to the diameter of the discharge orifice is 0.65 ($l_0 =$ 1.3 mm). Pressurized working fluids are fed into the chamber through the respective tangentially drilled inlets (d_p) and dispersed into the quiescent ambient air. The liquid flow rate (m_l) is kept constant at 7.95 g/s and the air pressures were gradually increased in steps as $m_a/m_l =$ 0.085−0.116. The PDPA is installed to specify the flows, providing the information on the individual particle size between 1 μm and 250 μm in this investigation. The focal lengths of the transmitting and receiving optics were 400 mm and 500 mm respectively. The radial profiles of a geometric sequence space were obtained at measurement locations of Z = 20, 30, 50, 80, 120, and 170 mm downstream from the nozzle. The droplet quantities were calculated by collecting 10,000 samples at each point. 10

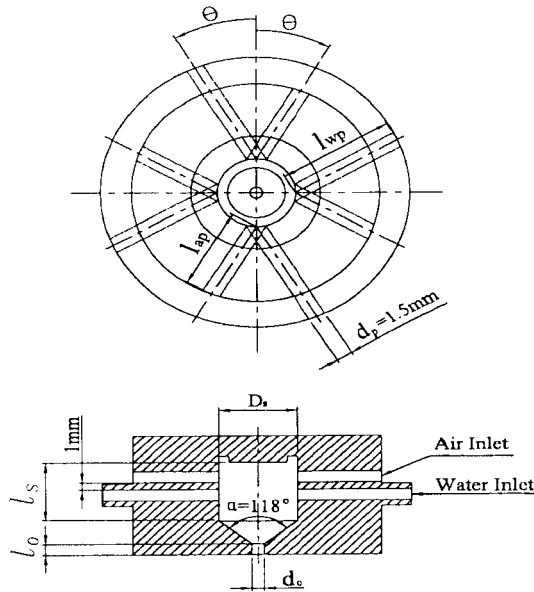*Corresponding author.* e-mail: rhobj@moak.chonbuk.ac.kr

Figure 1. Schematic diagram of the nozzle configuration.

Figure 2. Photographs illustrating the visualization: (a) ALR=0.085; (b) ALR=0.116.

seconds was set as the upper limit even though the sampling time depends on the local number density. Positive values of u (coordinate z) correspond to streamwise droplets moving in the downstream direction and positive values of v (coordinate y) signify radially outward motion from the spray centerline. The mean velocities and the rms values of the fluctuating quantities were normalized by the maximum velocities (um, the maximum axial velocity at a given location, or vm, the maximum radial velocity). Radius was non-dimensionalized by the half-value width of the velocity distribution. The half-velocity width, b, is the distance from the axis of a point where the mean streamwise velocity is half to its value on the streamwise axis.

3. RESULTS AND DISCUSSIONS

Figure 2 shows the photographic disintegration patterns of the sprays emanating from the atomizer with the liquid and the air counter-swirled. The liquid flow rate is kept by varying the air-to-liquid mass ratio from 0.085 for the case of Figure 2(a) and 0.116 for the Figure 2(b), respectively.

Several features of the flowfield in the primary breakup region are revealed. In the presence of higher air-to-liquid mass ratio, the dense core is seen to be surrounded by relatively higher streamwise velocities and persists comparatively farther downstream. However, it is apparent that there are no local void at all axial locations from the surroundings, which is probable to observe in the swirling cases. This is mainly attributed to the continuous and internal mixing phases even though
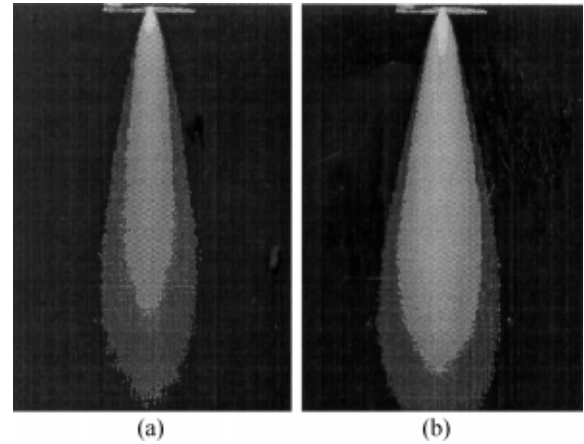
the twin fluids are counter-swirled.

It is observed that the spray angle increases slightly with increasing gas mass flow rate when compared with that of the lower one. Also, it indicates that the spray structure is totally different regardless of the gas flow rate from that of a pressure swirl atomizer that can be categorized as a hollow-cone spray. The pattern of spray droplets for the inner mixing part incarnated in white gets longer and wider for the higher air mass flow rate.

Figure 3 represent the mean axial velocity distributions in the radial direction for the different air-to-liquid mass ratio at seven measurement locations. The positive values of U indicate that the flow is moving downstream of the nozzle. The more or less bell shaped curves are seen to be geometrically similar and the velocity distributions are
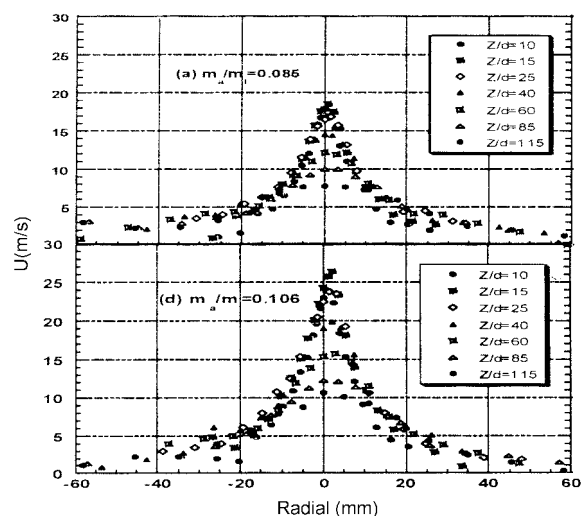

Figure 3. Variations of mean axial velocity along the radial distance.

highly symmetrical about the spray axis. The distributions show qualitative consistency even though there are some quantitative variations with increasing the air-to-liquid mass ratio. The axial velocity components are found to reach maxima in the spray center and reach a minimum near the spray boundary in this pneumatic atomizer.

When compared to the profile at Z/d=15, the velocities in the center at Z/d=10 are relatively lagging behind as shown in Figure 3 revealing the somewhat greater effect on droplets of the surrounding air drag force and the subsequent pushing effect in the spray leading edge. This can be attributed to the strong propagation due to the axial momentum in the center. Also, a drag force with decreasing momentum in the spray boundary is a perceptible ingredient to consider affecting on the spray droplets as the axial directions away from the nozzle exit. It is also found that there is only one pair of axial velocity peak in spite of introducing atomizing component in the swirl direction, when compared to the observation in pressure swirl atomizer having two pairs of peak (Rho *et al.*, 1998). But, beyond a radius of about 15 mm, no differences are apparent in velocities when compared to the spray center, which display nearly the same in spite of different additional atomizing air.

In an attempt to establish the generalities, non-dimensional axial velocity profile as a function of R/b from various spray conditions is shown in Figure 4. Radial profiles for the axial velocities from the present study correlate reasonably well with the other previous similarity formation, but the velocities are high near the spray periphery. This is due to the presence of modest swirl in the atomizing air, which increases the velocities at this spray periphery. It is found to be Gaussian in form on the jet axis. At all locations, it can be approximated by an
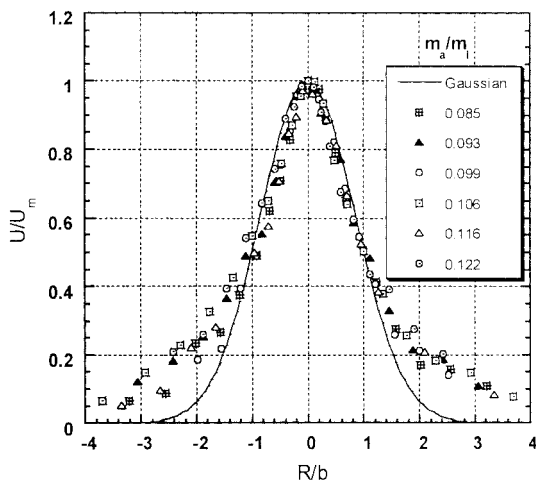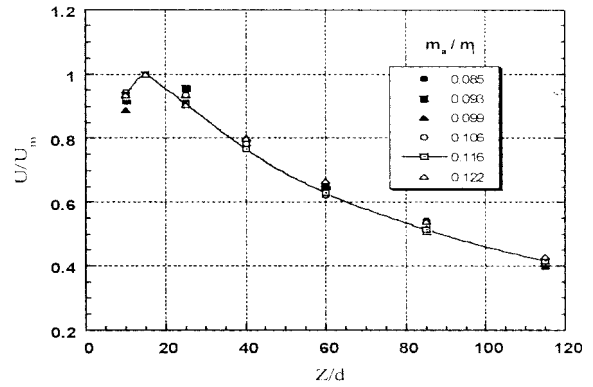

Figure 5. Nondimensional distribution of axial mean velocity along the axis.

identical distribution independent of air pressures. This can be sufficiently explained by taking into account the transfer of momentum from the central region to the periphery due to the inherent swirl. Also, this is evidently substantiated by the fact that the maximum values for the radial and tangential components are exhibited near the outer region away from the centerline. Accordingly, the spray trajectories in the peripheral region are wider.

Figure 5 illustrates the comparisons of normalized mean axial velocity along the central axis. It is interesting to see the fact that the maximum velocity in the leading spray tip (i.e., Z/d=10) have the lower value than that of the spray axis at a distance of Z/d=15 without regard to the air-to-liquid mass rate ratios.

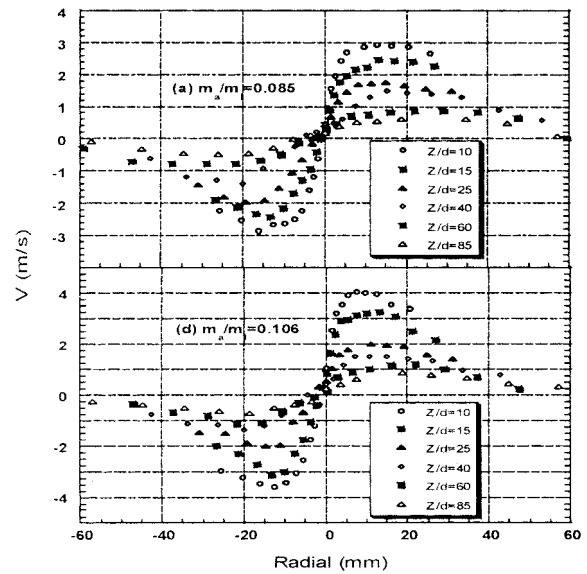Figure 4. Nondimensional axial velocity with various air/liquid mass.

Figure 6. Distribution of mean radial velocity along the axial distance.

The leading droplets are suddenly decelerated due to aerodynamical drag of the surrounding air. Those droplets following this leading edge have different aerodynamical interaction. This means that the droplet overtaking and the velocity acceleration of the leading spray edge may occur. That's why the droplet maximum velocity must exist in the axial distance of Z/d=15. Beyond the maximum value at Z/d=15, however, the axial velocity profile decreases abruptly along the downstream locations for all the conditions.

Radial variations in the mean radial velocities are presented in Figure 6. The radial velocity profiles show that the positive values of V indicate the outward flow, and that the negative values of V illustrate the inward flow from the spray periphery. The results reveal that the development of the velocity field has the expected similar trends with those observed for U at each axial location. As it gets closer to the spray periphery, the magnitude of V independent of the air/liquid mass ratio is considerably enhanced at around 10 mm away from the center. This rapid increase is attributed to the greater expansion of the spray that results from the swirling atomizing air. As a result, the radial momentum of the spray is strongly penetrated through the radial outward direction. The results show that the magnitude of the droplet mean radial velocity decays with increasing axial position for all the air/liquid mass ratios.

Profiles of swirl velocity between the higher and the lower air/liquid mass ratio are illustrated in Figure 7 for different axial locations. The positive values of W indicate the flow is moving in the counter-clockwise direction about the centerline. It is apparent that the tangential
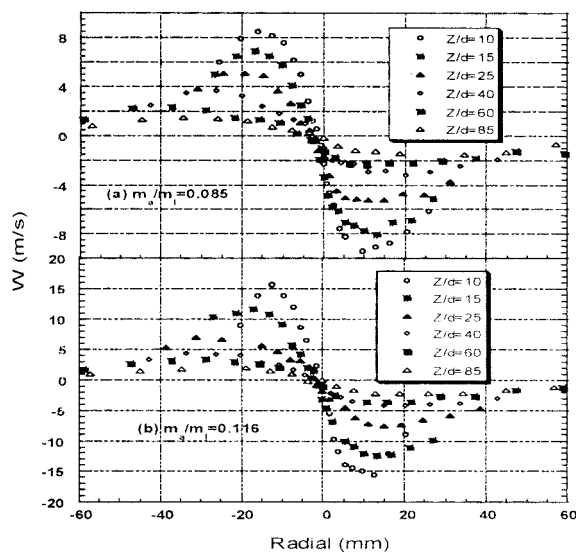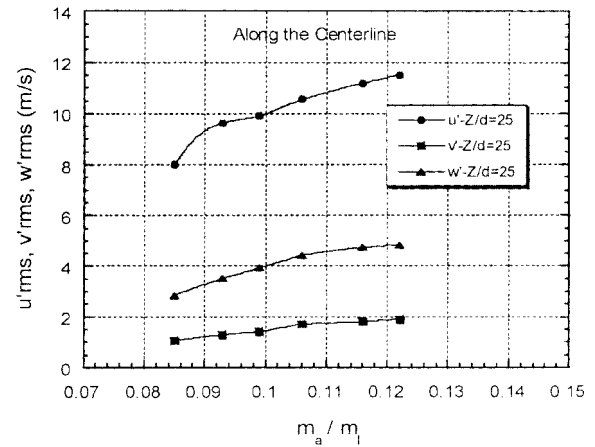

Figure 8. Variation of Fluctuating velocity as a function of air/liquid mass ratio.

velocities are considerably higher than the radial ones and as symmetric as previously observed for axial or radial velocities. It shows that the mean swirl velocity is well coincident with those obtained from the radial variations in terms of both the peak location and the decay with increasing the axial downstream. It shows that there is a strong swirling velocity in the upstream section

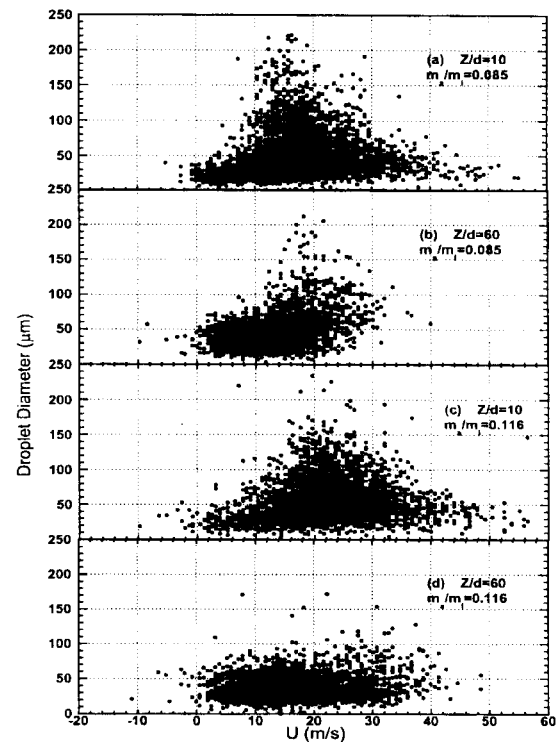Figure 7. Distribution of mean tangential velocity along the axial distance.

Figure 9. Velocity-Diameter correlation with different air/liquid mass ratio.

of spray and that it decreases in the downstream section. It is very interesting to observe that at most of the axial distances of downstream, the peak tangential velocities for the higher air/liquid mass ratio are nearly a factor of two higher those of the lower case.

This interesting increase can be observed due to the rapid expansion prompted by the substantial strong swirl components. Similar to the results shown for the radial velocities, the radial location for the peak mean tangential velocity is also shifted outward for all the cases. At every axial distances, the profiles have emerged to give a single tangential velocity peak near the spray periphery. An explanation for this is that the atomizing air is the only source of swirl momentum, which caused the spray droplets to be dispersed toward the spray periphery where the presence of tangential swirl has much impact.

The distributions of fluctuating velocities along the centerline as a function of air-to-liquid mass ratio are shown in Figure 8. Fluctuating tangential velocities are substantially greater than fluctuating radial velocities at all air to liquid mass ratios. At the axial down-stream distance of $Z/d=25$, the values of fluctuating axial velocity along the axis are highest at all conditions, while fluctuating radial values are lowest. Analysis for the

Figure 10. Variation of SMD with radial position at different axial locations.

droplet diameters disclosed that larger droplets consistently attained the higher mean and fluctuating velocities across the entire width of the spray than smaller droplets, which will be discussed in detail in the next segments.

Figure 9 shows the correlation pattern between velocity component and droplet diameters at upstream is still consistent with the downstream profiles. Although these correlations are qualitatively similar for both cases at each axial location, there are some notable differences. The effect of increasing the air/liquid mass ratio is to affect the correlation of velocity-diameter by widening the range of velocity components. Regardless of the mass ratio, it is also interesting to note that somewhat wider scattering droplets are omnipresent at upstream where it is associated with the droplet motion in the tangential direction than detected in the spray downs downstream. Moreover, it shows an apparent tendency of droplets for the higher air/liquid mass ratio to have larger axial velocity components and smaller droplet sizes than for the lower mass ratio. For example, the value of U is well correlated with diameter over the range 5 μm < D < 50 μm, whereas for D > 50 μm, the dependence of diameter on axial velocity appears to weaken sharply.

Figure 10 shows the variation of Sauter Mean Diameter along the axial downstream. It is quite interesting to consider that the droplets at upstream regions in the center are typically larger than those of off the axis. An initial increase of SMD may be due to the possibility of droplet coalescence that exists between droplets despite of strong axial momentum, showing that the SMD decreases from approximately 88-120 μm at $Z/d=15$ to 63 μm at $Z=85$ in the centerline. Note also that the profile at $Z/d=15-40$ exhibits a minimum in the spray boundary (i.e., it increases from 50–77 μm at $Z=15$ to 70 μm at $Z=85$ in the spray sheet region). This is attributed to the fact that droplets at upstream are presumably affected with the higher swirl components, which are displacing the bulk of the droplets radially outward from the center region. At $Z/d=40-85$, however, the maximum values of SMD in the spray periphery increase, which might be explained by the droplet entrainment from the outer part of the spray to the central region. Consequently, that the smaller diameters are less abundant near the spray boundary is attributed to the characteristic feature of internal mixing counterflowing nozzles. The SMD values decrease with an increase in air supply pressure by providing higher relative velocity at the interface of two-phase, and it is well established that SMD is inversely proportional to the relative velocity.

4. CONCLUSIONS

The following specific observations provide valuable insight into the flow behavior and atomization characteri-
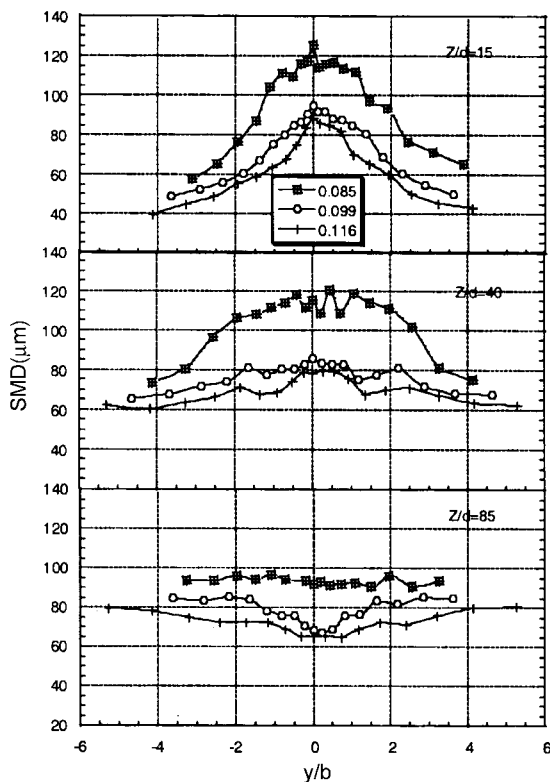
stics regarding the sprays issued from the counterflowing nozzle. The photographic visualization showed that the spray angle increased slightly with increased air/liquid mass ratio due to the radial growth rate. However, the axial, radial and tangential velocity components are found to be symmetric about the axis and showed qualitative consistency. The velocities in the leading edge are lagging behind, which explained the surrounding air drag and the subsequent pushing effect. Also, the nondimensional velocity profiles showed an identical distribution with a Gaussian curve in the spray center region. But, the phenomenon in the outer region revealed the wider distribution, substantiating the swirl effect. The magnitude in SMD near the center is noticeably larger than that of off the axis, which can be explained by the droplet coalescence and too strong axial momentum. Also, the SMD is inversely proportional to the air supplied pressure.

REFERENCES

Dodge, L. G. and Moses, C. A. (1984). A study of the breakup and atomization of a combusting diesel fuel spray, *20th Symposium International on Combustion*, The Combustion Institute, Pittsburgh, 1239.

Eroglu, H. and Chigier, N. (1991). Initial drop size and velocity distributions for airblast coaxial atomizers, *J. of Fluids Engineering*, Sep., **113**, 453–459.

Lefebvre, A. H. (1992). *Twin-Fluid Atomization: Factors Influencing Mean Drop Size, Atomization and sprays*, 101–119.

Presser, C., Avedisian, C. T., Hodges, J. T. and Gupta, A. K. (1996). *Behavior of droplets in pressure-atomized fuel sprays with coflowing air swirl, Progress in Astronautics and Aeronautics*, **2**, Chap. 2, 31–62.

Rho, B. J., Kang, S. J., Lee, S. G. and Oh, J. H. (1998). Swirl effect on the spray characteristics of a twin-fluid jet, *KSME International Journal*, **12**(5), 899–906.

Takahashi, F. and Schmoll, W. J. (1995). Characteristics of a velocity modulated pressure swirl atomizing spray, *J. of Propulsion and Power*, **11**(5), Sep.-Oct., 955–962.